



## Detecting coevolution of positively selected in turtles sperm-egg fusion proteins

Jinxu Dong, Hui Jiang, Lei Xiong, Jiawei Zan, Jianjun Liu, Mengli Yang, Kai Zheng, Ziming Wang, Liuwang Nie\*

Provincial Key Lab of the Conservation and Exploitation Research of Biological Resources in Anhui, Life Science College of Anhui Normal University, Wuhu, Anhui, China



### ARTICLE INFO

#### Keywords:

Sperm-egg fusion  
Tu-Izumo1  
Tu-JUNO  
Tu-CD9  
Hybridization

### ABSTRACT

Physically interacting sperm-egg proteins have been identified using gene-modified animals in some mammal species. Three proteins are essential for sperm-egg binding: Izumo1 on the sperm surface, and JUNO and CD9 on the egg surface. Most proteins linked to reproductive function evolve rapidly among species by positive selection, and have correlated evolutionary rates to compensate for changes on both the sperm and egg. Up to now, interactions between sperm and egg proteins have not been identified in non-mammalian vertebrates, such as turtles that have interspecific hybrids that can produce surviving F1 generations. To explore the potential physical interactions of sperm-egg proteins in turtle species, the coding region of *Izumo1*, *JUNO*, and *CD9* homologous genes (named *Tu-Izumo1*, *Tu-JUNO*, and *Tu-CD9*) in six turtle species (*Mauremys reevesii*, *M. mutica*, *M. sinensis*, *Cistoclemmys flavomarginata*, *Platysternon megacephalum* and *Chrysemys picta bellii*) were identified, amplified, and sequenced, and tissue-specific expression was analyzed in *M. reevesii*. We constructed phylogenetic trees and analyzed the signatures of coevolution between sperm-egg protein pairs using MirrorTree Server and linear regression methods. The results showed that Tu-Izumo1, Tu-JUNO, and Tu-CD9 proteins have correlated evolutionary rates, and that the area where Tu-Izumo1 interacts with Tu-JUNO has only one positive selection site in some turtle species. These results suggest there is a potential interaction between Tu-Izumo1 and Tu-JUNO among turtles that can interbreed, and that a significantly lower positive selection in the interaction region may be one of the reasons why turtle hybrids are so common. Further studies are required to uncover Tu-Izumo1, Tu-JUNO and Tu-CD9 protein biological functions during gamete fusion.

### 1. Introduction

Fertilization is an important part of the sexual reproduction process, which involves interactions between reproduction proteins (Jin et al., 2011). At the present, the molecular mechanisms of fertilization process are not yet clear; however, some proteins that are essential for sperm-egg fusion in mammals, have been identified using gene-modified animals (e.g., such as Izumo1 on the sperm surface, and JUNO and CD9 on the egg surface) (Aydin et al., 2016). The way they work has also been elucidated. During fertilization, Izumo1 (a monomer that originally existed in the acrosome) is exposed on the sperm surface and recognizes the Izumo1 counter-receptor (a monomeric JUNO on the surface of the oocyte) initiating sperm-egg adhesion. Izumo1 finally becomes a dimer and loses affinity to JUNO (Inoue, 2014; Inoue et al., 2005). CD9 is a molecule involved in the binding of sperm and egg that attaches to the binding site of Izumo1 and JUNO (Bianchi et al., 2014; Chalbi et al., 2014; Sutovsky, 2009). There is recent evidence showing that

hybridization is common in animals, especially in turtles (Dai et al., 2013; Godwin et al., 2014; Xia et al., 2011). According to previous research, 22 unique interspecies pairs (fields or farms) were found within Bataguridae, which can hybridize and produce an F1 generation (Table S1) (Dai et al., 2013; Pan et al., 2009; Xia et al., 2011). It is obvious that the sperm and eggs of the parents involved in hybridization can recognize each other. It is thus necessary to explore whether interacting sperm-egg proteins are subsistent and whether they have direct or indirect interactions with each other during fertilization in turtles.

Interacting sperm-egg proteins, are among the most rapidly evolving classes of proteins driven by positive selection (Swanson and Vacquier, 2002). A major cause of this phenomenon is the coevolution of sperm and egg proteins (Clark et al., 2009). If the fertilization protein changes, the partner protein changes too, thereby the fertilization proteins can maintain species-specificity at the level of sperm-egg fusion. In addition, the amino-acid residues in their binding interface

\* Corresponding author at: College of Life Sciences, Anhui Normal University, No.1 Beijing East Road, Wuhu 241000, Anhui Province, China.  
E-mail address: [lwnie@mail.ahnu.edu.cn](mailto:lwnie@mail.ahnu.edu.cn) (L. Nie).

would be positively selected (Claw et al., 2014). Therefore, the potential interaction between sperm-egg proteins can be predicted by searching for the correlation of evolutionary rates between them (Grayson, 2015; Vicens and Roldan, 2014).

In this study, the coding regions of *Izumo1*, *JUNO*, and *CD9* homologous genes (*Tu-Izumo1*, *Tu-JUNO*, and *Tu-CD9*) of six turtle species were identified, amplified and sequenced by RT-PCR. qPCR was used to verify whether they were expressed in specific tissues in *M. reevesii*. Then, we reconstructed protein phylogenetic trees based on each protein individually and compared the amino acid sequences of *Tu-Izumo1*, *Tu-JUNO*, and *Tu-CD9*. The MirrorTree Server (Ochoa and Pazos, 2010) and linear regression analysis were used to estimate coevolution between these proteins. In addition, the numbers of amino acids targeted by positive selection in *Tu-Izumo1*, *Tu-JUNO*, and *Tu-CD9* were also analyzed. Our aims were to predict and analyze potential interactions between *Tu-Izumo1*, *Tu-JUNO*, and *Tu-CD9*, and to speculate on the possible reasons for the prevalence of turtle hybridization at the sperm-egg binding protein level, through the search of similar evolutionary histories in a group of closely-related turtle species.

## 2. Material and methods

### 2.1. Animals and ethics

Six species for sequencing *Tu-Izumo1*, *Tu-JUNO*, and *Tu-CD9* gene were *M. reevesii*, *M. mutica*, *M. sinensis*, *C. flavomarginata*, *P. megacephalum* and *C. picta bellii*, in which the first five species have overlapping distribution in the southeast of China and the latter is from the pet market in Wuhu, Anhui Province, China. The coding region sequences of the remaining species (*Malaclemys terrapin terrapin*, *Terrapene mexicana triunguis*, *Gopherus agassizii*, *Chelonia mydas*, *Pelodiscus sinensis* and *Alligator mississippiensis*) were retrieved from NCBI (National Center for Biotechnology Information), see Table S2.

Procedures involved in animals and their care were consistent with NIH guidelines (NIH Pub. No. 85-23, revised 1996) and approved by the Animal Care and Use Committee of Anhui Normal University under approval number #20170705.

### 2.2. *Tu-Izumo1*, *Tu-JUNO*, and *Tu-CD9* coding sequence amplification and sequencing using RT-PCR methods

Total RNA was extracted from the testis and ovary of turtles by the TRIzol reagent (Promega, Madison, USA). Then, single-stranded cDNA was reverse-transcribed using the Fast Quant RT Kit with gDNase (Tiangen, Beijing, China). Three genes coding sequences (*Tu-Izumo1*, *Tu-JUNO*, and *Tu-CD9*) from start codons to stop codons were amplified from cDNA products with specific primer pair (see Table 1). PCR amplification was performed in total volumes of 50  $\mu$ L with 100 ng cDNA, 20  $\mu$ M of each primer, 8  $\mu$ L dNTPs, 25  $\mu$ L 2  $\times$  GC Buffer I and 2.5 U TaKaRa LA Taq. The PCR conditions were as follows: one cycle of 5 min at 95  $^{\circ}$ C; 36 cycles of denaturation at 95  $^{\circ}$ C for 30 s; 30 s at the appropriate annealing temperature; and extension at 72  $^{\circ}$ C for 90 s; followed by one cycle of 10 min at 72  $^{\circ}$ C. After amplification, PCR products were purified, cloned and sequenced. And BLASTN (<https://blast.ncbi.nlm.nih.gov/Blast.cgi>) was used to compare the sequences (Table S2).

### 2.3. Construction of phylogenetic trees based on the amino acid sequences of *Tu-Izumo1*, *Tu-JUNO*, and *Tu-CD9*

In order to test whether these proteins (*Tu-Izumo1*, *Tu-JUNO*, and *Tu-CD9*) are undergoing the same evolutionary trajectories, phylogenetic trees based on the amino acid sequences of these proteins were constructed respectively with the maximum likelihood (ML) and the Bayesian inference (BI) methods. In each amino acid databases, the sequence alignment was carried out using MAFFT (Katoh et al., 2017). The ML analyses were conducted in RAxML v.8.2.10 with rapid bootstrap for 1000 replicates under PROTGAMMAAUTO model. In Bayesian analyses, we used the parameter aamodelpr = mixed, and then four chains were run for 1,000,000 generations using random initial trees, and every 1000 generations were sampled (Guindon et al., 2010; Ronquist and Huelsenbeck, 2003). In this study, *A. mississippiensis* was used as the outgroup.

### 2.4. Tissue specific expression analysis of *Tu-Izumo1*, *Tu-JUNO*, and *Tu-CD9* in *M. reevesii* using qPCR methods

The sexual maturation three female and three male samples were analyzed, and each sample have three technical triplicates. The relative expression levels of *Tu-Izumo1*, *Tu-JUNO*, and *Tu-CD9* mRNA were determined using total RNA extracted from heart, liver, intestine, muscle, testis and ovary of *M. reevesii*. Relative gene expression levels were assessed via Roche LightCycler 480 real-time PCR cyclers (Bio-Rad, Hercules, CA, USA) and SuperReal PreMix Plus (SYBR Green) kit (Tiangen, Beijing, China), according to the manufacturer's protocols. The relative gene expression levels were calculated using the  $2^{-\Delta\Delta CT}$ , and *gapdh* as reference gene. The primers (Table 2) used to assay gene expression were designed using Oligo 7. The qPCR conditions were as follows: 95  $^{\circ}$ C for 30 s, followed by 40 cycles of denaturation at 95  $^{\circ}$ C for 5 s, 63  $^{\circ}$ C for 20 s, and then a final melting curve from 65  $^{\circ}$ C to 95  $^{\circ}$ C to assess that single products were amplified by the qPCR reaction.

### 2.5. Analysis of three-dimensional protein structure of *Tu-Izumo1*, *Tu-JUNO*, and *Tu-CD9*

Protein three-dimensional structure models for *Tu-Izumo1*, *Tu-JUNO*, and *Tu-CD9* were simulated based on the structure models of homolog sequences were provided by the SWISS-MODEL (<https://www.swissmodel.expasy.org/>) (Bienert et al., 2017) and download from PDB database. Then protein structures were visualized and analyzed using the Java and PyMOL v.0.99rc2 program.

### 2.6. Tests of positive selection of *Tu-Izumo1*, *Tu-JUNO*, and *Tu-CD9*

The positive selection sites of *Tu-Izumo1*, *Tu-JUNO*, and *Tu-CD9* proteins of 11 species were tested by using the Codeml tool implemented in PAML package v4.9 (Yang, 2007) to run the site model and branch-site model with the null model M7, the alternative model M8 (Yang, 2007; Yang et al., 2005) and a third test compared the likelihood of the model M8 to the likelihood of a null model M8a in which  $\omega$  was fixed to 1 in avoidance of detecting false signatures of positive selective as a result of functional relaxation (Wong et al.,

**Table 1**  
primers used to clone the genes in this study.

	Primer (5'-3')	Annealing temperature
<i>Tu-Izumo1</i> -cd-sense	GCTATGGCTTGGGCACTGTGGCT	64 $^{\circ}$ C
<i>Tu-Izumo1</i> -cd-antisense	CATCCTTCTCTGGCACCTCCTGCT	
<i>Tu-JUNO</i> -cd-sense	AGATGGCTGCTCCTTTGGGCTGTGCT	53 $^{\circ}$ C
<i>Tu-JUNO</i> -cd-antisense	TCAGAGCAGGACCCAGGAGAGCAG	
<i>Tu-CD9</i> -cd-sense	GCAGGGCAGTCAGAGGAAT	59 $^{\circ}$ C
<i>Tu-CD9</i> -cd-antisense	TGGAAGGCATGTGGCAAGACTAA	

**Table 2**  
Real-time PCR primer sequences in the experiment.

	Primer (5'-3')	Annealing temperature
<i>Tu-Izumo1</i> -RT-sense	GGGCGCATGGTTCACCACT	62 °C
<i>Tu-Izumo1</i> -RT-antisense	GTGACCATGACCTGCTCCGAGC	
<i>Tu-JUNO</i> -RT-sense	GCCAGTGTGCTCTGTGGAAAG CAGGTTGGGCGAGCACTCGT	60 °C
<i>Tu-JUNO</i> -RT-antisense		
<i>Tu-CD9</i> -RT-sense	CTTTTAGGAAGTGCAGTCC CAGTATAGAAGTTTGAATTGT	52 °C
<i>Tu-CD9</i> -RT-antisense		
<i>Tu-GAPDH</i> -RT-sense	AGCTGCCCTCAACTCTAGCAA	55 °C
<i>Tu-GAPDH</i> -RT-antisense	AACTCCGTGGATTCTACAACA	

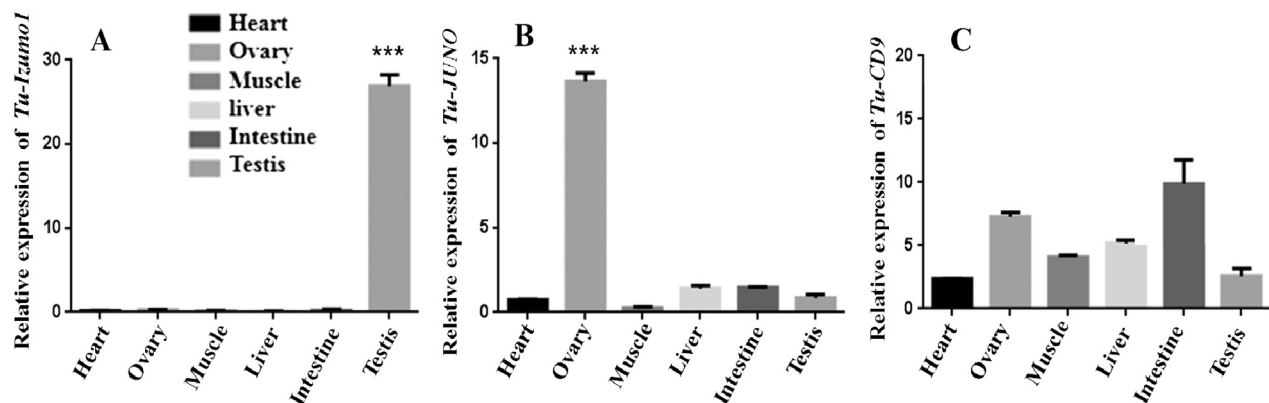


**Fig. 1.** Real-time reverse transcriptase-polymerase chain reaction (RT-PCR) analyses of (A) *Tu-Izumo1*, (B) *Tu-JUNO* and (C) *Tu-CD9* expression quantities in *M. reevesii* heart, ovary, muscle, liver, intestine and testis (mean  $\pm$  S.D.; n = 3). Asterisk (\*\*\*) is statistically significant ( $P < 0.01$ ).

2004). Then we analyzed the positive selection identified by empirical Bayes values  $> 0.95$ .

### 2.7. Analyses of coevolution among *Tu-Izumo1*, *Tu-JUNO*, and *Tu-CD9*

To test whether three proteins show correlated evolutionary rates across turtle species, 11 species turtles were analyzed by two different methods. The first way is based on the MirrorTree Server (<http://csbg.cnb.csic.es/mtserver/index.php>) by the 'From multiple alignments' from provided protein alignments, and using the 'From trees' to analyze the same RAxML trees used for PAML analyses (Ochoa and Pazos, 2010; Waterhouse et al., 2009). If the correlation value is  $> 0.800$ , it represents the existence of strong correlations between this pair proteins (Pazos and Valencia, 2001). The second method is that we performed linear regression analyses among root-to-tip  $\omega$  ratios of *Tu-Izumo1*, *Tu-JUNO*, and *Tu-CD9*. And the average  $\omega$  values from the root of the tree to each terminal species tip (root-to-tip  $\omega$  ratios) were calculated using branch site model implemented in Codeml (PAML package v4.9). Linear regressions were conducted with R x64 3.4.4.

## 3. Results

### 3.1. The coding region of *Tu-Izumo1*, *Tu-JUNO*, and *Tu-CD9* gene in turtles

Complete coding sequences of *Tu-Izumo1*, *Tu-JUNO* and *Tu-CD9* genes were obtained for six turtle species by RT-PCR. All sequences were the translated to proteins using universal genetic codes. The protein *Tu-Izumo1*, containing an Izumo domain and an Izumo-Ig domain, is composed of 272 amino acids. The protein *Tu-JUNO* consists of 245 amino acids, and contains a folate-receptor domain. The protein *Tu-CD9*, harboring four extracellular transmembrane domains, is formed by 223 amino acids (Fig. S1). Since these proteins share the same functional domain with mammalian *Izumo1*, *JUNO*, and *CD9*, we named them *Tu-Izumo1*, *Tu-JUNO*, and *Tu-CD9* for turtle species.

### 3.2. Phylogenetic analyses of *Tu-Izumo1*, *Tu-JUNO*, and *Tu-CD9*

Discrepancies in topology were observed between the results of the maximum likelihood and the Bayesian approach for *Tu-Izumo1*, *Tu-JUNO*, and *Tu-CD9* phylogenies (Figs. S2, S3, and S4). Moreover, none of the trees showed a topology that was in agreement with the phylogeny trees of the species (Fig. S5) (Zhou et al., 2015). The clade grouping the most highly related species (*M. reevesii*, *M. sinensis* and *M. mutica*) for *Tu-JUNO* phylogeny could not be resolved with significant bootstrap value and posterior probability in *Tu-Izumo1* and *Tu-CD9* phylogeny. The phylogenetic position of the *P. megacephalum* was controversial in three phylogenetic trees. The discordance observed between phylogenetic trees constructed from amino acid sequences and species trees suggests that *Tu-Izumo1*, *Tu-JUNO*, and *Tu-CD9* are undergoing independent evolutionary trajectories regarding to the historical relationships between the species, which is possibly due to these genes are subject to directional selective pressures. Similar results have been reported in rodents by Vicens and Roldan (2014).

### 3.3. *Tu-Izumo1* and *Tu-JUNO* are expressed specifically in the gonads

The results of real-time RT-PCR show that *Tu-Izumo1* was expressed specifically in testis, which is consistent with the expression of *Izumo1* in mammals (Inoue et al., 2005; Kim et al., 2013). *Tu-JUNO* had ovary-specific expression. These results indicate *Tu-Izumo1* and *Tu-JUNO* could have a reproductive function. However, no tissue-specific expression was detected for *Tu-CD9*, although, its expression in the intestine was slightly higher than that in other tissues (Fig. 1).

### 3.4. Positive selection test of *Tu-Izumo1*, *Tu-JUNO*, and *Tu-CD9*

*Tu-Izumo1*, *Tu-JUNO*, and *Tu-CD9* in turtles appear to be evolving under positive selection and the LRTs (M8 vs M7 and M8 vs M8a) were in favor of the selection model (Table 3). There was one positively selected site in *Tu-Izumo1* ( $\omega_{(M8)}$  ratio = 1.976), and three positively

**Table 3**  
Tests of positive selection for Tu-Izumo1, Tu-JUNO and Tu-CD9.

Gene	N	LRT <sub>(M7vsM8)</sub>	LRT <sub>(M8vsM8a)</sub>	$\omega_{(M8)}$	BEB sites
Tu-Izumo1	11	12.23**	11.08**	1.976	1; 274P*
Tu-JUNO	11	33.65**	33.66**	1.365	3; 36E*, 164I*, 191T*
Tu-CD9	11	33.35**	33.06**	3.993	12; 113E*, 124K*, 144Y**, 151M**, 152L**, 154T**, 155V**, 160Q**, 169S*, 172F*, 174V*, 179A*

LRTs, likelihood-ratio tests; N, number of compared lineages; Likelihood ratio test values are presented in columns M7 versus M8 and M8 versus M8a. M7 allows  $\omega$  to vary between 0 and 1; M8a (M7 with  $\omega = 1$ ) is the null hypothesis for M8 (Yang, 2007). The total number of BEB sites with probability > 0.5 are reported. BEB sites were only produced for clades evolving under positive selection.

\*  $P > 95\%$ .

\*\*  $P > 99\%$ .

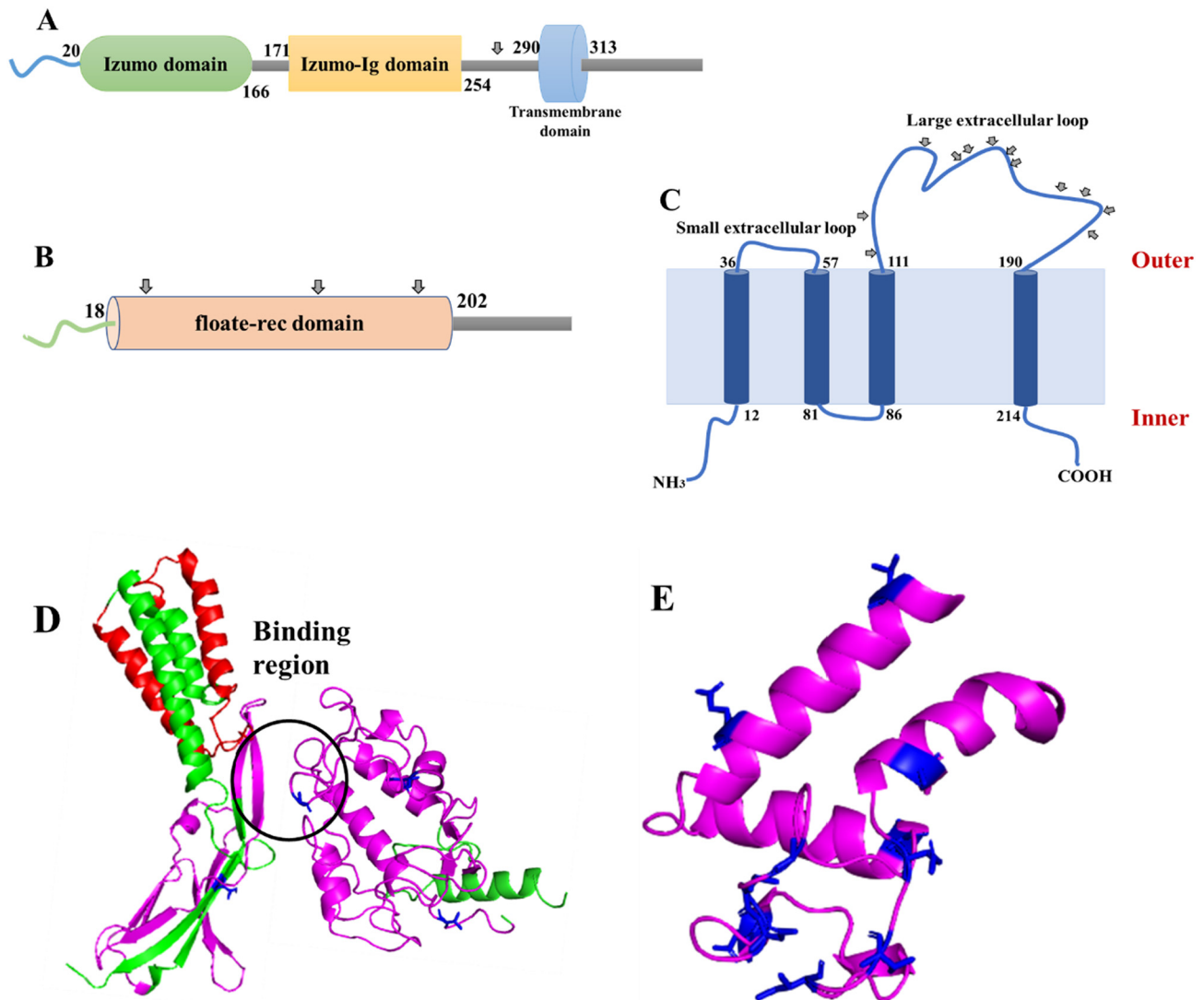


**Fig. 2.** Tu-Izumo1, Tu-JUNO and Tu-CD9 protein structure. A: Scheme of Tu-Izumo1 representing the known domains. B: Scheme of Tu-JUNO representing the known domain. C: Scheme of Tu-CD9 representing the distribution of positively selected residues in the large extracellular loop. Arrowheads indicating the position of amino acids under positive selection. D: Crystal structure of Tu-Izumo1 (PDB ref. 5f4v.1.A) and Tu-JUNO (PDB ref. 5izq.1.A), red and magenta regions represent the functional domain. E: Three-dimensional-structural model based on the crystal structure of human CD81 extracellular domain (PDB ref. 5tcx.1.A), and sites under positive selection are shown as blue sticks.

selected sites in Tu-JUNO (with an average  $\omega_{(M8)}$  ratio = 1.365); a total of 12 positively selected sites were identified in the Tu-CD9 alignment (with an average  $\omega_{(M8)}$  ratio = 3.993).

There was only one site of positive selection detected by molecular evolutionary analyses in the extracellular region of the Tu-Izumo1 protein; this is significantly lower than the 15 sites found in rodents (Vicens and Roldan, 2014), 101 sites in mammals, and 65 sites in

Laurasiatheria (Grayson, 2015) (Fig. 2A). And the positive site is neither in Izumo domain nor in Izumo-Ig domain. Therefore, the Izumo and Izumo-Ig domains are relatively conserved. There were three amino acid sites under positive selection located at the folate-receptor domain of the Tu-JUNO protein (positions 19–201) (Fig. 2B), which is slightly lower than the number of positive selection sites previously found in mammals. This domain is an essential region for gamete recognition

**Table 4**  
MirrorTree Server identifies lineage-specific signals of coevolution between Tu-Izumo1, Tu-JUNO and Tu-CD9 in turtles.

	n	Correlation value from tree	p-Value	Correlation value from MSA	p-Value
(Tu-Izumo1)-(Tu-CD9)	9	0.959	< 0.000001	0.914	< 0.000001
(Tu-Izumo1)-(Tu-JUNO)	9	0.956	< 0.000001	0.827	< 0.000001

MSA: multiple sequence alignments. Italicized correlation values lie above the MirrorTree correlational cut-off of 0.800 and are suggestive of coevolution between this pair proteins.

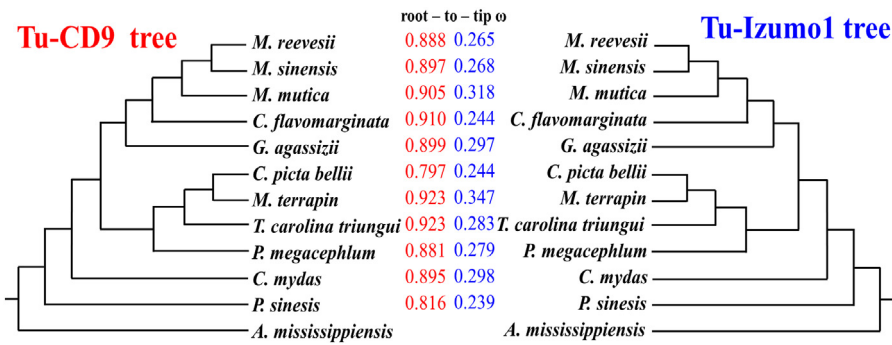


**Fig. 3.** Evolutionary rates of Tu-CD9 and Tu-Izumo1. Tree topology was reconstructed based on reported turtles phylogenies (Zhou et al., 2015). Lineage-specific ω values were calculated for each terminal branch and averaged from the last common ancestor to each species.

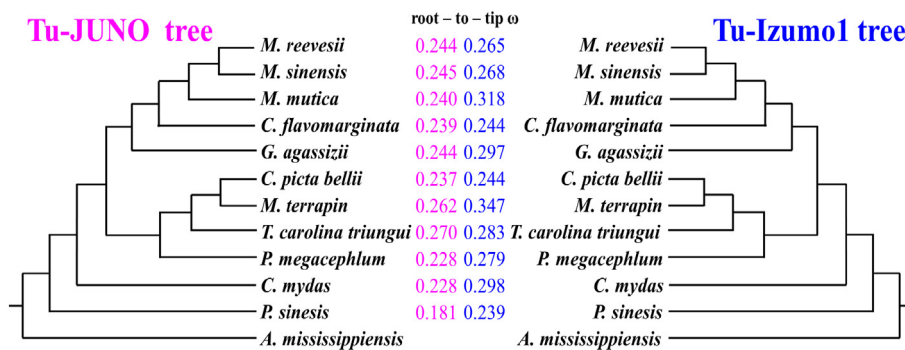


**Fig. 4.** Evolutionary rates of Tu-JUNO and Tu-Izumo1. Tree topology was reconstructed based on reported turtles phylogenies (Zhou et al., 2015). Lineage-specific ω values were calculated for each terminal branch and averaged from the last common ancestor to each species.

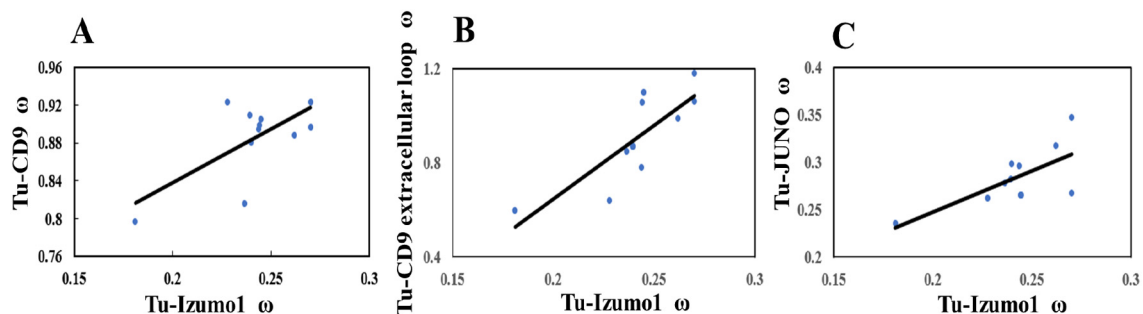


**Fig. 5.** Coevolution among Tu-Izumo1, Tu-JUNO and Tu-CD9. A: Coevolution between Tu-Izumo1 and Tu-CD9; B: coevolution between Tu-Izumo1 and Tu-CD9 extracellular loop ω; C: coevolution between Tu-Izumo1 and Tu-JUNO. The ω values estimated for nine turtles are plotted.

(Bianchi et al., 2014). There was only one positive selection site in the (Tu-Izumo1)-(Tu-JUNO) binding region (Fig. 2D), suggesting lower positive pressure in turtles. Twelve amino acids showing significant positive selection in the Tu-CD9 protein were detected in the large extracellular loop (Fig. 2C). These residues were at positions 110–190 of Tu-CD9, which are involved in sperm-egg fusion (Fig. 2E) (Zhu et al., 2002). Thus, positive selection in the large extracellular loop of Tu-CD9 may have important functions in sperm-egg fusion.

### 3.5. Coevolution among Tu-Izumo1, Tu-JUNO, and Tu-CD9 in turtles

The ‘From multiple alignments’ and ‘From trees’ approach on the MirrorTree Server identified a robust signal of correlated evolutionary rates between Tu-Izumo1, Tu-JUNO, and Tu-CD9 (Table 4; Figs. 3 and 4). In addition, the average ω values from the root of the tree to each terminal species tip of *Tu-Izumo1*, *Tu-JUNO*, and *Tu-CD9* have been estimated. A significant positive correlation between Tu-Izumo1 and Tu-CD9 root-to-tip ω ratios was obtained (F = 6.1974, P = 0.0345) (Fig. 5A). Given that the large extracellular loop of Tu-CD9 showed the

strongest signals of positive selection, we evaluated whether the divergences of the region of Tu-CD9 drive the coevolution of Tu-CD9 and Tu-Izumo1. We estimated root-to-tip  $\omega$  ratios using alignments of the extracellular loop of Tu-CD9 and Tu-Izumo1, a significant positive correlation was obtained ( $F = 17.827$ ,  $P = 0.0022$ ) (Fig. 5B). We also sought for signatures of coevolution in Tu-Izumo1 and Tu-JUNO; root-to-tip  $\omega$  ratios of Tu-Izumo1 showed a positive relationship as they were correlated with Tu-JUNO ( $F = 7.9292$ ,  $P = 0.0202$ ) (Fig. 5C). These results support the hypothesis that Tu-Izumo1, Tu-JUNO, and Tu-CD9 are experiencing coordinated evolution in turtles.

We also tested the coevolution between Tu-Izumo1, Tu-JUNO, and Tu-CD9 based on the topologies of trees derived from an alignment that included Tu-Izumo1, Tu-JUNO, and Tu-CD9 amino acid sequences by maximum likelihood and Bayesian inference methods (Supplemental Fig. S6). Regression between  $\omega$  estimates of Tu-Izumo1, Tu-JUNO, and Tu-CD9 was statistically significant, maximum likelihood tree: (Tu-Izumo1)-(Tu-JUNO) was  $F = 6.3121$ ,  $P = 0.0332$ ; (Tu-Izumo1)-(Tu-CD9) was  $F = 5.0184$ ,  $P = 0.0414$ . Bayesian inference tree: (Tu-Izumo1)-(Tu-JUNO) was  $F = 6.9708$ ,  $P = 0.0269$ ; (Tu-Izumo1)-(Tu-CD9) was  $F = 5.1414$ ,  $P = 0.0496$ . These results indicate that the correlation of the evolutionary rates of Tu-Izumo1, Tu-JUNO, and Tu-CD9 is not influenced by phylogenetic relationships between species.

#### 4. Discussion and conclusion

##### 4.1. Quantitative expressive of Tu-Izumo1, Tu-JUNO, and Tu-CD9

Although Izumo1 and JUNO are absolutely essential for gamete fusion in mammals (Kim, 2015; Kim et al., 2013), their expression pattern in other species remains unknown. Our analysis indicated that Tu-Izumo1 is expressed specifically in the testis of turtles. Tu-JUNO displayed ovary-specific expression, which could indicate a reproductive function similar to JUNO in mammals. Our observations suggest Tu-Izumo1 and Tu-JUNO exist in the testis and the ovary, respectively, and that they might be contributing to sperm-egg fusion in turtles. In addition, due to its various biological functions (e.g., promoting cell activation and differentiation), Tu-CD9 was expressed in all tissues, which is consistent with previous studies (Erovic et al., 2003; Hori et al., 2004; Kwon et al., 2017).

##### 4.2. Coevolution of Tu-Izumo1, Tu-JUNO, and Tu-CD9

Coevolution of sperm-egg binding proteins has been previously reported in rodents and primates (Claw et al., 2014; Vicens and Roldan, 2014), but has never been reported in turtles. Our results show correlated evolution between these three proteins. Previous studies have shown that correlated evolution can occur between proteins with the same function and/or tissue-specific expression or that interact physically (Clark et al., 2012). *Tu-Izumo1* and *Tu-JUNO* displayed tissue-specific expression in turtles, so we hypothesize that correlated evolutionary rates are a result of these proteins having the same function or of their interaction. Recent studies show that Izumo1 and JUNO can interact directly in mammals (Bianchi et al., 2014). We speculate that Tu-Izumo1 and Tu-JUNO can also interact directly in turtles in sperm-egg binding, because they are coevolving and have the same evolutionary rate, but it is not known for sure until further functional tests are done.

It is interesting that Tu-CD9 shows higher evolutionary rates than Tu-Izumo1 and Tu-JUNO, and subjects to higher positive selection pressure (Claw et al., 2014). The reasons detailed below can explain the phenomenon. CD9 only plays a regulatory role in the interaction between Izumo1 and JUNO, and collaborates with JUNO in mammals (Bianchi et al., 2014). CD9 is expressed in multiple tissues and cells, and has many physiological functions, including important immune functions. Recent findings indicate that genes with immune function, such as, antimicrobial peptide genes, often have higher rates of evolution

than those with no immune functions (Erler et al., 2014).

##### 4.3. The possible reason for hybridization success in turtle

There are many reported cases of crossbreeding between *M. reevesii*, *M. sinensis*, *M. mutica* and *C. flavomarginata*, such as *M. reevesii*  $\times$  *M. mutica* (Mccord, 1997), *M. sinensis*  $\times$  *M. reevesii* (Xia et al., 2011) and *C. trifasciata*  $\times$  *M. mutica* (Pan et al., 2009), which have overlapping geographical distribution. No events of hybridization between *P. megacephalum* with *M. reevesii*, *M. sinensis*, *M. mutica* and *C. flavomarginata* have been reported, although they have overlapping distributions or hybridization between *C. picta bellii* with them, due to differences karyotypes and rather distant phylogenetic relationships.

There is a long-standing hypothesis that rapid evolution and positive selection observed in interacting proteins are often caused by coevolution between sperm and egg proteins to avoid hybridization (Grayson, 2015; Vicens and Roldan, 2014). In our results, although there was evident correlated evolution among the three proteins, there was only one positive selection site in the area where Tu-Izumo1 binds to Tu-JUNO. This will reduce the barriers of reproductive isolation. Furthermore, previous studies have reported that if the protein structure from one species is similar to that of another species, it may interact with the partner protein in other species (Bianchi and Wright, 2015; Inoue et al., 2013). In this study, we found that the turtles that can interbreed are more closely related to each other than to the other turtles that cannot. Hence, we speculate that closer affinity between *M. reevesii*, *M. sinensis*, *M. mutica* and *C. flavomarginata*, and lower selection pressure of the binding area of Tu-Izumo1 and Tu-JUNO, may be one of the reasons for interbreeding. It is thus necessary to explore whether interacting sperm-egg proteins are subsistent and whether they have direct or indirect interactions during fertilization in turtles.

Our results show for the first time that Tu-Izumo1 and Tu-JUNO have tissue-specific expression in turtles, and predict interactions between sperm-egg binding proteins based on the characterization of their coevolution in turtles even though the mechanisms of their interactions and the molecular role of these proteins during sperm-egg interaction are not yet clear. Furthermore, positive selection sites of these three proteins, imply that the few positive selection sites in the sperm-egg binding region may be the reasons for interspecies hybridization.

#### Acknowledgements

This research was supported by the National Natural Science Foundation of China (NSFC, No. 31372198), the Research Fund of the Key Laboratory of Biotic Environment and Ecological Safety of Anhui Province, and the Key Laboratory of Biomedicine in Gene Diseases and Health of Anhui Higher Education Institutes, Anhui Normal University.

#### Appendix A. Supplementary data

Supplementary data to this article can be found online at <https://doi.org/10.1016/j.mod.2019.02.001>.

#### References

- Aydin, H., Sultana, A., Li, S., Thavalingam, A., Lee, J.E., 2016. Molecular architecture of the human sperm Izumo1 and egg JUNO fertilization complex. *Nature* 534 (7608), 562–565. <https://doi.org/10.1038/nature18595>.
- Bianchi, E., Wright, G.J., 2015. Cross-species fertilization: the hamster egg receptor, Juno, binds the human sperm ligand, Izumo1. *Philos. Trans. R. Soc. Lond.* 370 (1661), 20140101. <https://doi.org/10.1098/rstb.2014.0101>.
- Bianchi, E., Doe, B., Goulding, D., Wright, G.J., 2014. Juno is the egg Izumo receptor and is essential for mammalian fertilization. *Nature* 508 (7497), 483–487. <https://doi.org/10.1038/nature13203>.
- Bienert, S., Waterhouse, A., Beer, Tjaart A.P., Tauriello, G., Studer, G., Bordoli, L., Schwede, T., 2017. The SWISS-MODEL repository—new features and functionality. *Nucleic Acids Res.* 45 (1), 313–319. <https://doi.org/10.1093/nar/gkw1132>.
- Chalbi, M., Barraudlange, V., Ravoux, B., Howan, K., Rodriguez, N., et al. 2014. Binding of sperm protein Izumo1 and its egg receptor Juno drives Cd9 accumulation in the

- intercellular contact area prior to fusion during mammalian fertilization. *Development*, 141 (19), pp. 3732–3739. doi:<https://doi.org/10.1242/dev.111534>.
- Clark, N.L., Gasper, J., Sekino, M., Springer, S.A., Aquadro, C.F., Swanson, W.J., 2009. Coevolution of interacting fertilization proteins. *PLoS Genet.* 5 (7), e1000570. doi:<https://doi.org/10.1371/journal.pgen.1000570>.
- Clark, N.L., Alani, E., Aquadro, C.F., 2012. Evolutionary rate covariation reveals shared functionality and coexpression of genes. *Genome Res.* 22 (4), 714–720. doi:<https://doi.org/10.1101/gr.132647.111>.
- Claw, K.G., George, R.D., Swanson, W.J., 2014. Detecting coevolution in mammalian sperm–egg fusion proteins. *Mol. Reprod. Dev.* 81 (6), 531–538. doi:<https://doi.org/10.1002/mrd.22321>.
- Dai, S., Yabe, T., Hikida, T., 2013. Hybridization between *Mauremys japonica* and *Mauremys reevesii* inferred by nuclear and mitochondrial DNA analyses. *J. Herpetol.* 48 (4), 445–454. doi:<https://www.jstor.org/stable/43287471>.
- Erlor, S., Lhomme, P., Rasmont, P., Lattorff, H.M.G., 2014. Rapid evolution of antimicrobial peptide genes in an insect host–social parasite system. *Infect. Genet. Evol.* 23 (2), 129–137. doi:<https://doi.org/10.1016/j.meegid.2014.02.002>.
- Erovic, B. M., Pammer, J., Hollemann, D., Woegerbauer, M., Geleff, S., Fischer, M. B., et al. 2003. Motility-related protein-1/CD9 expression in head and neck squamous cell carcinoma. *Head Neck*, 25 (10), pp. 848–857. doi:<https://doi.org/10.1002/hed.10306>.
- Godwin, J.C., Lovich, J.E., Ennen, J.R., Kreiser, B.R., Folt, B., Lechowicz, C., 2014. Hybridization of two megacephalic map turtles (Testudines: Emydidae: Graptemyd) in the Choctawhatchee River drainage of Alabama and Florida. *Copeia* 2014 (4), 725–742. doi:<https://doi.org/10.1643/CH-13-132>.
- Grayson, P., 2015. Izumo1 and Juno: the evolutionary origins and coevolution of essential sperm–egg binding partners. *R. Soc. Open Sci.* 2 (12), 150296. doi:<https://doi.org/10.1098/rsos.150296>.
- Guindon, S., Dufayard, J.-F., Lefort, V., Anisimova, M., Hordijk, W., Gascuel, O., 2010. New algorithms and methods to estimate maximum-likelihood phylogenies: assessing the performance of PhyML 3.0. *Syst. Biol.* 59 (3), 307–321. doi:<https://doi.org/10.1093/sysbio/syq010>.
- Hori, H., Yano, S., Koufujii, K., Takeda, J., Shirouzu, K., 2004. CD9 expression in gastric cancer and its significance. *J. Surg. Res.* 117 (2), 208–215. doi:<https://doi.org/10.1016/j.jss.2004.01.014>.
- Inoue, N., 2014. The Mechanism of Sperm–Egg Fusion in Mouse and the Involvement of IZUMO1. *Sexual Reproduction in Animals and Plants*. Springer, Tokyo, pp. 393–399. doi:[https://doi.org/10.1007/978-4-431-54589-7\\_32](https://doi.org/10.1007/978-4-431-54589-7_32).
- Inoue, N., Ikawa, M., Isotani, A., Okabe, M., 2005. The immunoglobulin superfamily protein Izumo is required for sperm to fuse with eggs. *Nature* 434 (7030), 234–238. doi:<https://doi.org/10.1038/nature03362>.
- Inoue, N., Hamada, D., Kamikubo, H., Hirata, K., Kataoka, M., Yamamoto, M., Hagihara, Y., 2013. Molecular dissection of IZUMO1, a sperm protein essential for sperm–egg fusion. *Development* 140 (15), 3221–3229. doi:<https://doi.org/10.1242/dev.094854>.
- Jin, M., Fujiwara, E., Kakiuchi, Y., Okabe, M., Satouh, Y., Baba, S.A., Hirohashi, N., 2011. Most fertilizing mouse spermatozoa begin their acrosome reaction before contact with the zona pellucida during in vitro fertilization. *Proc. Natl. Acad. Sci. U. S. A.* 108 (4), 4892–4896. doi:<https://doi.org/10.1073/pnas.1018202108>.
- Katoh, K., Rozewicki, J., Yamada, K.D., 2017. MAFFT online service: multiple sequence alignment, interactive sequence choice and visualization. *Brief. Bioinform.* doi:<https://doi.org/10.1093/bib/bbx108>.
- Kim, E., 2015. Molecular cloning and characterization of Izumo1 gene from bovine testis. *J. Anim. Sci. Technol.* 57 (1), 1–7. doi:<https://doi.org/10.1186/s40781-015-0049-1>.
- Kim, E., Kim, J.S., Lee, Y., Song, B.S., Sim, B.W., Kim, S.U., Chang, K.T., 2013. Molecular cloning, characterization of porcine IZUMO1, an IgSF family member. *Reprod. Domest. Anim.* 48 (1), 90–97. doi:<https://doi.org/10.1111/j.1439-0531.2012.02037.x>.
- Kwon, H.J., Choi, J.E., Su, H.K., Son, Y., Bae, Y.K., 2017. Prognostic significance of CD9 expression differs between tumor cells and stromal immune cells and depends on the molecular subtype of the invasive breast carcinoma. *Histopathology* 70 (7), 1155–1165. doi:<https://doi.org/10.1111/his.13184>.
- Mccord, W.P., 1997. *Mauremys pritchardi*, a new batagrid turtles from Myanmar and Yunnan, China. *Chelon. Conserv. Biol.* 2, 555–562.
- Ochoa, D., Pazos, F., 2010. Studying the co-evolution of protein families with the MirrorTree web server. *Bioinformatics* 26 (10), 1370–1371. doi:<https://doi.org/10.1093/bioinformatics/btq137>.
- Pan, D.B., Chen, K.C., Zhu, X.P., Zheng, G.M., Liu, Y.H., Chen, Y.L., Li, K.B., 2009. The morphologic characters of hybrid (*Mauremys mutica* ♀ × *Cuora trifasciata* ♂) and comparison with their parents. *Acta Hydrobiol. Sin.* 33 (4), 620–626. doi:<https://doi.org/10.3724/SP.J.1035.2009.40620>.
- Pazos, F., Valencia, A., 2001. Similarity of phylogenetic trees as indicator of protein–protein interaction. *Protein Eng.* 14 (9), 609–614. doi:<https://doi.org/10.1093/protein/14.9.609>.
- Ronquist, F., Huelsenbeck, J.P., 2003. MrBayes 3: Bayesian phylogenetic inference under mixed models. *Bioinformatics* 19 (12), 1572–1574. doi:<https://doi.org/10.1093/bioinformatics/btg180>.
- Sutovsky, P., 2009. Sperm–egg adhesion and fusion in mammals. *Expert Rev. Mol. Med.* 11 (4), e11. doi:<https://doi.org/10.1017/S1462399409001045>.
- Swanson, W.J., Vacquier, V.D., 2002. The rapid evolution of reproductive proteins. *Nat. Rev. Genet.* 3 (2), 137–144. doi:<https://doi.org/10.1038/nrg733>.
- Vicens, A., Roldan, E.R., 2014. Coevolution of positively selected IZUMO1 and CD9 in rodents: evidence of interaction between gamete fusion proteins? *Biol. Reprod.* 90 (5), 113. 1–9. doi:<https://doi.org/10.1095/biolreprod.113.116871>.
- Waterhouse, A.M., Procter, J.B., Martin, D.M., Clamp, M., Barton, G.J., 2009. Jalview version 2—a multiple sequence alignment editor and analysis workbench. *Bioinformatics* 25 (9), 1189–1191. doi:<https://doi.org/10.1093/bioinformatics/btp033>.
- Wong, W.S.W., Yang, Z., Goldman, N., Nielsen, R., 2004. Accuracy and power of statistical methods for detecting adaptive evolution in protein coding sequences and for identifying positively selected sites. *Genetics* 168 (2), 1041–1051. doi:<https://doi.org/10.1534/genetics.104.031153>.
- Xia, X., Wang, L., Nie, L., Huang, Z., Jiang, Y., Jing, W., Liu, L., 2011. Interspecific hybridization between *Mauremys reevesii* and *Mauremys sinensis*: evidence from morphology and DNA sequence data. *Afr. J. Biotechnol.* 10 (35), 6716–6724. doi:<https://doi.org/10.5897/AJB11.063>.
- Yang, Z., 2007. PAML 4: phylogenetic analysis by maximum likelihood. *Mol. Biol. Evol.* 24 (8), 1586–1591. doi:<https://doi.org/10.1093/molbev/msm088>.
- Yang, Z., Wong, W.S.W., Nielsen, R., 2005. Bayes empirical Bayes inference of amino acid sites under positive selection. *Mol. Biol. Evol.* 22 (4), 1107–1118. doi:<https://doi.org/10.1093/molbev/msi097>.
- Zhou, H., Yuan, J., Nie, L., Yin, H., Li, H., Dong, X., Huang, Z., 2015. The historical speciation of *Mauremys sensu lato*: ancestral area reconstruction and interspecific gene flow level assessment provide new insights. *PLoS One* 10 (12), e0144711. doi:<https://doi.org/10.1371/journal.pone.0144711>.
- Zhu, G.Z., Miller, B.J., Boucheix, C., Rubinstein, E., Liu, C.C., Hynes, R.O., Primakoff, P., 2002. Residues SFQ (173–175) in the large extracellular loop of CD9 are required for gamete fusion. *Development* 129 (8), 1995–2002. doi:<http://dev.biologists.org/content/129/8/1995.long>.